 doi:10.20944/preprints202210.0352.v1

Article

Impact of Lithologic Heterogeneity on Brittleness of Cenozoic Mixed Fine-grained Sedimentary Rock Reservoirs in Western Qaidam Basin

Xiang Li [a, b]*, Kunyu Wu [c, d], Jiangong Wang [b], ShaoYong Yang [d], Qinghui Zhang [d] and Qiang Zhang [b]

[a] School of Geoscience and Technology, Southwest Petroleum University, Chengdu, Sichuan 610500, China;
[b] PetroChina Research Institute of Petroleum Exploration & Development-Northwest, Lanzhou, Gansu, China 730020;
[c] School of Petroleum and Natural Gas Engineering, Southwest Petroleum University, Chengdu, Sichuan 610500, China;
[d] Research Institute of Exploration and Development of PetroChina Qinghai Oilfield Company, Dunhuang, Gansu, China 73620;

Abstract: In order to understand the impact of lithologic heterogeneity of continental mixed fine-grained sedimentary rocks on reservoir brittleness in western Qaidam basin, the mechanical properties of the rocks and their correlation with mineral composition and petrographic characteristics were studied by measns of mineralogy, petrography and triaxial stress test. The results show that the reservoir rocks can be divided into 5 different types according to the mechanical properties of the reservoir (characteristics of stress-strain curves), among them Type I and III belong to similar elastoplastic failure model, type II shows a special pulse failure mode for plastic material, type IV shows a failure mode of mixed characteristics, and type V exhibits a typical plastic failure model. The correlation between minerals and mechanical properties indicates that quartz and feldspar, which are often considered brittle minerals, do not contribute much to the brittleness of continental fine-grained sedimentary rocks. The main minerals affecting reservoir brittleness are dolomite and clay minerals, and their contributions to reservoir brittleness are positive and negative, respectively. The petrographic analysis results prove that the abnormal correlation between rock mechanical properties and quartz and feldspar is caused by the different rock fabrics. When dolomite forms a rock skeleton, it typically exhibits greater strength, brittleness and physical properties than other minerals. Based on the results, a brittleness evaluation standard for continental fine-grained sedimentary rock reservoir is proposed, and the validity of the standard is verified by the spatial correlation between the lithology probability model and the micro-seismic monitoring data, indicating that the spatial heterogeneity of dolomite-rich rock is the main controlling factor for the development of 'sweet spot' in the Cenozoic continental fine-grained sedimentary rock reservoir in the Western Qaidam Basin.

Keywords: lithologic heterogeneity; rock-mechanical property; mixed carbonate; tight reservoirs; Qaidam basin

1. Introduction

During the past decades, the increasing global consumption of hydrocarbon energy has triggered the booming of unconventional oil and gas studies. Moreover, in North America, the success of large-scale commercial development of shale gas from Barnett, Antrim, Marcellus, Woodford, etc. (Curtis, 2002; Montgomery et al., 2005; Jarvie et al., 2007) and development of tight oil from Bakken, Eagle Ford, Wolfcamp etc. (Montgomery, 1996; Sonnenberg and Pramudito, 2009; Kuhn et al., 2012; Hentz et al., 2013; Fairbanks et al., 2016; Aderibigbe et al., 2016) has led to a significant unconventional oil & gas revolution, which fundamentally reformed the global energy framework (Yergin, 2011; EIA,

 doi:10.20944/preprints202210.0352.v1

2013). Since 2010, drawing on the experience of North America, China's oil and gas industry has gradually expanded its exploration targets from traditional traps to unconventional areas, realizing the economic development of marine shale gas and continental shale oil and gas in China (Yangzhi, 2019; Guoxin Li, 2020; Wenzhi Zhao, 2020).

Many scholars have promoted a further understanding on the sedimentary and reservoir characteristics, hydrocarbon generation potential and accumulation mechanism of continental fine-grained sedimentary rocks including organic-rich shale (Shaomin Zhang., 2018; Yuan Deng., 2019; Le Li., 2019; Lihong Zhou., 2019). The continental fine-grained sedimentary rocks are quite different from conventional marine shale oil. Sedimentary rocks with a particle size of less than 0.1 mm and a content of more than 50% are generally defined as fine-grained sedimentary rocks (Caineng Zou, et al., 2013). Shale is a kind of fine-grained sedimentary rock with sheet-like or lamellar bedding structure composed of debris, clay and organic matter with a particle size of less than 0.0039mm (Maowen Li et al., 2019). It is well known that a stable wide and slow tectonic setting is a necessary condition for the formation and enrichment of Marine shale oil in North America (Tyson R V, et al., 1991). While the continental sedimentary system in China is significantly different from the marine basin in North America in terms of basin scale, tectonic stability and sedimentary type (Maowen Li, 2019). Due to the combined influence of tectonic action, frequent provenance supply and turbulent lake level, the mixed fine-grained sedimentary rocks composed of mudstone, terrigenous clasts and carbonate minerals formed the main continental unconventional reservoirs (Lihong Zhou et al., 2018, 2019). The Porosity is generally less than 10% and permeability is less than $1x10^{-3}$ μm^2 (Du., 2014; Bodziak et al., 2014; Dong et al., 2017). The development ages of continental fine-grained sedimentary rocks covered from the Upper Paleozoic Permian to the Neogene, and the sedimentary environment includes terrestrial fresh water, brackish water, salt water and alkaline water (Maowen Li er al., 2022).

In addition to basic research on lithology, lithofacies, and source rocks in the preliminary stage, the development methods and engineer parameters of continental fine-grained sedimentary rocks are also very important. Among them, the massive hydraulic fracturing has been the most effective and primary method for reservoir stimulation (Bustin and Bustin, 2012; Sone and Zoback, 2013; Bodziak et al., 2014). Variation in rock fabric and mineral compositions causes different responses of reservoirs to hydraulic fracturing, as the strain accommodation of reservoir rocks changes with lithological types and fabric (Bodziak et al., 2014; Dong et al., 2017). Therefore, it is necessary not only to accurately map the mechanical facies of the entire reservoir, but also to understand the mechanical facies changes and properties of the reservoir rocks whose mineral composition varies greatly as a result of depositional changes.

In general, with the relative increase of clay mineral content, the limit strain that the formation can withstand before hydraulic fracturing takes effect also increases (Donath, 1970; Ferrill and Morris, 2008), indicating that mineral composition is the main but not all controlling factor of the rock mechanical properties of the reservoir. When the rock type changes, the strain adaptability of the formation at the buried depth may exceed the capacity of hydraulic fracturing. Published works indicate that previous researchers focused mainly on quantifying mechanical properties to understand the corresponding variables that a particular lithology can withstand before failure. Therefore, strain is a key factor to quantitatively describe the mechanical behavior of rocks during the processes of hydraulic fracturing. In practice, it is usually described in various terms, such as ductility (Donath, 1970; Ferrill and Morris, 2008), brittleness (Rickman et al., 2008), and hydraulic fracturability (Enderlin et al., 2011; Clemons et al., 2012), etc. Among them, the term 'brittleness' has been frequently used in the evaluation of mechanical properties of unconventional reservoir rocks (Geng et al., 2016; Li et al., 2018).

The first public discourse about brittleness index focused on the brittle mineral components (Bishop, 1967; Jarvie et al., 2007; Buller et al., 2010). Soon, the ratio of compressive strength to tensile strength is used to evaluate the brittleness of the rock, that is, the larger the ratio, the higher the brittleness (Hucka and Das, 1974). With further research, the

Preprints (www.preprints.org) | NOT PEER-REVIEWED | Posted: 24 October 2022 doi:10.20944/preprints202210.0352.v1

Young's modulus and Poisson's ratio are considered as two key parameters for rock brittleness characterization (Rickman et al., 2008), that is, the high Young's modulus and low Poisson's ratio correspond to high brittleness (Rickman et al., 2008; Labani and Rezaee, 2015). Moreover, the effect of pore fluid on the mechanical properties of rock was also widely discussed, that is, pore fluid increases the plasticity of rock and reduces brittleness (Heidari et al., 2014; Paul et al., 2017; Tan Wen-hui et al., 2018). At present, rock brittleness has been a comprehensive definition, which is generally evaluated through rock fracture characteristics, rock mineral composition, rock mechanical properties and pore fluid (Li et al., 2018). Comprehensive application of multiple methods promotes the accuracy of rock brittleness evaluation, such as rock mechanics analysis of rock samples, log data calculation and 3D seismic data inversion, etc. (Goodway et al., 2006; Mullen et al., 2007; Rickman et al., 2008).

In any case, stress-strain characteristics and mineral composition are still the most important indicators of brittleness. In the triaxial stress test of rocks, the stress–strain curve is divided into pre-peak and post-peak stages. The pre-peak stage generally represents the stable state, while the post-peak stage refers to an unstable state due to cracks (Tan Wen-hui., 2018). The post-peak sharp drop behavior represents the significant brittleness (Tarasov and Potvin, 2013). A series of brittle–plastic models have been used to study the post-peak stress drop in rocks and describe the instability after failure. The stress drop coefficient is also an important index to evaluate the brittleness (Ge et al., 1997; Zheng et al., 1997; Shi et al., 2006). The evaluation of rock brittleness is inherently complicated, and the complexity of continental mixed fine-grained sedimentary rocks undoubtedly increases the difficulty of evaluation of brittleness. In this paper, the internal relationship between mineral compositions, rock fabric and mechanical properties is systemically studied and conclusions will provide references to the hydraulic fracturing and engineering sweet spot choosing of reservoirs.

2. Geological setting

The Qaidam basin is a large continental intermountain hydrocarbon-bearing basin in northwest China, with ~12×10^4 km^2 of sedimentary rocks distributed in the basin (Fig. 1a). The basin is dominated by Cenozoic strata, and seismic exploration data show that the maximum thickness of the Cenozoic strata is more than 10000 m. Since the Early Cenozoic, the orogenic activities of the Eastern Kunlun Mountains and Altun Mountains have derived migration of the depositional center of Qaidam Basin from the west to the east (Lu and Xiong, 2009; Fu et al., 2016). The Cenozoic strata in the study area was subdivided into 5 stratigraphic units based on the lithology, paleontology and paleomagnetism, etc. From early toThey are the Lulehe formation ($E_{1\text{-}2}l$), the Xiaganchaigou formation ($E_{2\text{-}3}xg$), the Shangganchaigou formation (E_3-N_1sg), the Xiayoushashan formation (N_1xy), and the Shangyoushashan formation (N_1sy) (Fig. 1c, Table 1).

The Upper Member of the Xiaganchaigou formation ($E_{2\text{-}3}xg^2$) is the target strata of this study, which deposited in a saline lacustrine environment and is further subdivided into marginal (shore) sub-environment and pelagial sub-environment (Wang et al., 2020). The main sedimentary environment in study area ($E_{2\text{-}3}xg^2$) is the pelagial subenvironment, which is characterized by typical mixed fine-grained sedimentary rocks. (Fig. 1b). The mixed fine-grained sedimentary rocks are characterized by high-frequency interbedded organic-rich laminated shale and carbonate (Guoxin Li., 2022). In addition, terrigenous clastic carried by extra buoyancy provided by the saline water contribute to the complex mineral compositions of local carbonate rocks. The core samples in the study area are mainly migmatites of carbonate, mudstone and evaporite, including some clastic rocks of gravity flow origin. The main pore type in target layers is inter-crystalline pores formed by dolomitization, while the other pore types (such as inter-granular pores, dissolution pores, etc.) were less developed (Zhang et al., 2018). Reservoir matrix porosity is extremely low due to the fine-grained character and strong heterogeneity of mixed fine-grained sedimentary rocks. The statistical results of analysis data show that the distribution peaks of

Preprints (www.preprints.org) | NOT PEER-REVIEWED | Posted: 24 October 2022 doi:10.20944/preprints202210.0352.v1

porosity and permeability of reservoir are 3.1%~11.5% and 0.05~0.62 μm², respectively (Zhang et al., 2018). All these disadvantages result in a low or complete loss of natural production capacity of such reservoirs, further challenging the anthropogenic stimulation of reservoirs. The red rectangle in Figure 1b is the study area, which is a typical lacustrine mixed fine-grained sedimentary rocks. The study of this area is of great significance to reveal the characteristics of the same type of reservoir.

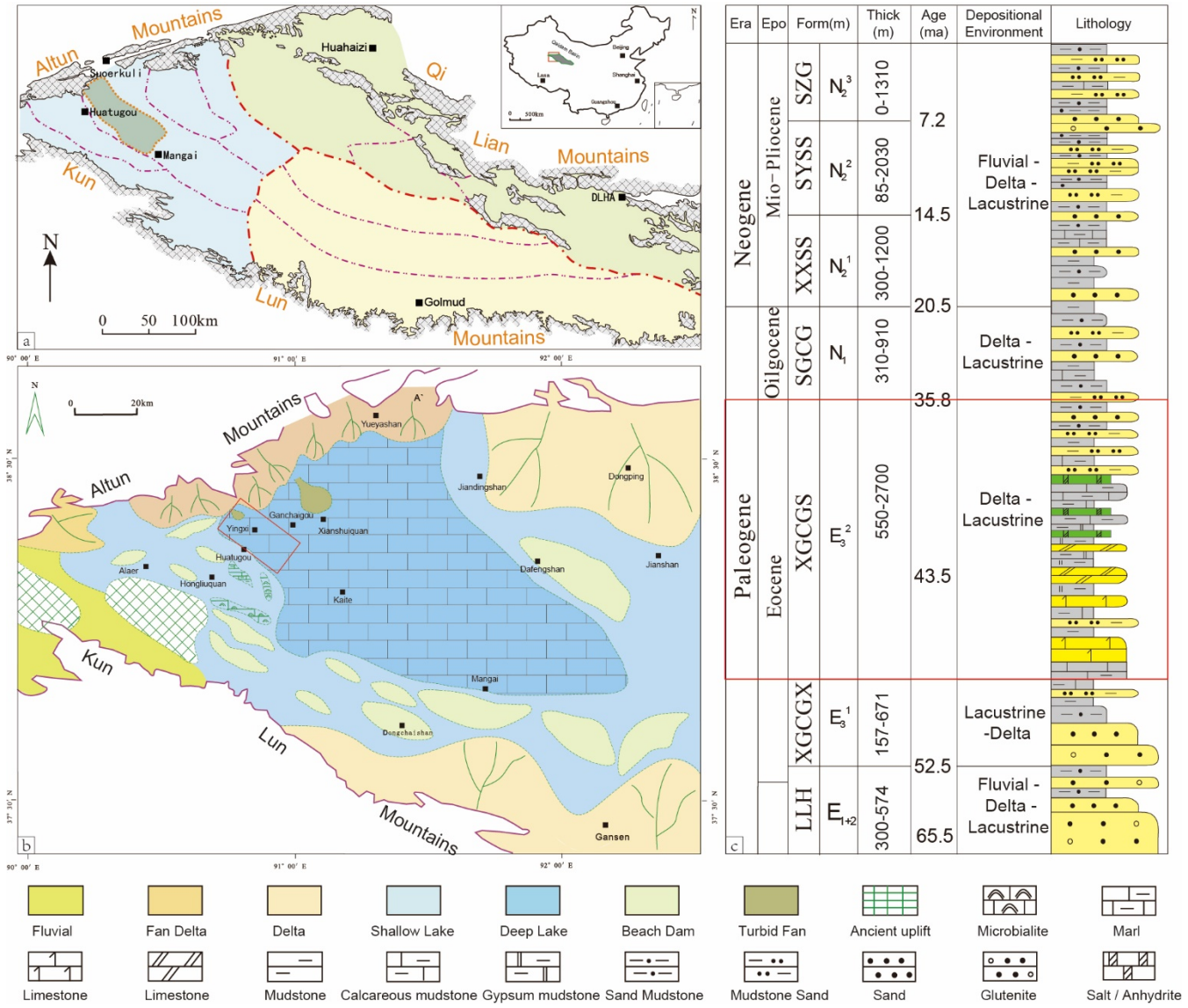

Figure 1. Tectonic location and topography of the study area. a- tectonic division of Qaidam basin; b- the topography of the study site.

Table 1. Stratigraphy division of Cenozoic in Qaidam basin.

Stratigraphic system				Symbol	Lithology
System	Series	Formation	Member		
Neogene	Miocene	Shangyoushashan		N_1sy	Predominated by brown-yellow sandy mudstone, with some argillaceous siltstone and conglomerate interbeds.
		Xiayoushashan		N_1xy	Red-brown mudstone and sandy mudstone, with some brown-red siltstone and calcareous mudstone inter-beds.
		Shangganchaigou		E_3-N_1sg	

Preprints (www.preprints.org) | NOT PEER-REVIEWED | Posted: 24 October 2022 doi:10.20944/preprints202210.0352.v1

Paleogene	Oligocene				Gray mudstone and siltstone develop in the lower part, while the upper part is predominated by brown-yellow mudstone and fine sandstone.
	Eocene	Xiaganchaigou	Upper	$E_{2\text{-}3}xg^2$	Predominated by dark-grey argillaceous-lime dolostone, lime dolostone, dolomitic limestone and calcareous mudstone, some anhydrite-rich beds and halite beds develop in the upper part.
			Lower	$E_{2\text{-}3}xg^1$	Brown-red mudstone with some grey-white fine sandstone and calcareous mudstone interbeds.
	Paleocene	Lulehe		$E_{1\text{-}2}l$	The brown-red conglomerate, conglomeratic sandstone, sandstone with some mudstone and sandy mudstone interbeds.

3. Sampling, data preparation and methodology

3.1. Triaxial experiment

In order to understand the impact of lithologic heterogeneity on the mechanical properties of the reservoir, 10 rock samples with different mineral compositions and fabrics were selected from drilling cores at a depth of 3860 - 4210 m in the Upper Member of Xiaganchaigou Formation. All samples were drilled using a 2.5 cm diameter core bit and then cut into cylindrical plugs ~5 cm in length. Prior to analysis, plunger samples were rinsed with the Soxhlet distillation-extraction apparatus and solvent mixture of chloroform/ methanol. After 48 hours of distillation-extraction, then all plunger samples were dried in an oven for 24 hours. The temperature and pressure parameters for this experiment were determined from in-situ measurements obtained from temperature and pressure sensors at the bottom of the well. The strata temperature of the rock samples ranges from 108 ~118 ℃, and the confining pressure is ~ 50 MPa (Table 2). Taking into account the consistency with the geological conditions and the upper limit of the temperature conditions of the experimental equipment, the temperature conditions of these experiments were all set to 100 ℃

Table 2. Core plug samples and tested conditions.

Sample ID	Depth /m	Length /mm	Diameter /mm	Sectional area /cm²	Volume /cm³	Cell pressure /MPa
1-44-1	4078.37	51.28	24.79	4.83	24.75	51.03
5-47-1	4122.64	48.53	24.81	4.83	23.46	51.54
12-3-1	3860.48	48.52	24.87	4.86	23.57	48.35
8-27-1	4146.50	48.03	24.75	4.81	23.11	51.83
2-126-1	4096.66	48.37	24.72	4.80	23.21	51.24
4-1-1	4106.75	50.39	24.72	4.80	24.18	51.36
12-8-1	3861.30	46.71	24.77	4.82	22.51	48.34
16-3-1	4202.26	48.05	24.88	4.86	23.36	52.54
9-36-1	3794.30	47.17	24.76	4.81	22.71	47.47
5-6-1	3766.90	46.88	24.79	4.83	22.63	47.16

The triaxial stress tests were performed on the triaxial stress test platform of the State Key Laboratory of Oil & Gas Reservoir Geology and Exploitation Engineering. The experimental equipment is RTR-1000 static/dynamic state triaxial rock mechanics servo test system of GCTS Company in the United States (Fig. 2). In the triaxial test, when the deformation rate signal fed back by the rock sample is inconsistent with the predetermined signal, the servo controller generates a corresponding comparison signal to push the servo to change the oil supply model, ensuring the deformation rate in a controllable range. When the rock samples begin to rupture, the deformation process shows a decrease in the bearing capacity and an increase in the deformation rate. As the deviator stress reaches

Preprints (www.preprints.org) | NOT PEER-REVIEWED | Posted: 24 October 2022 doi:10.20944/preprints202210.0352.v1

the tensile strength limit of the rock samples, the servo controller will actively close the servo valve to reduce the oil supply and rock test pressure. Thus, the test system will overcome the bursting phenomenon and obtain the specific deformation information.

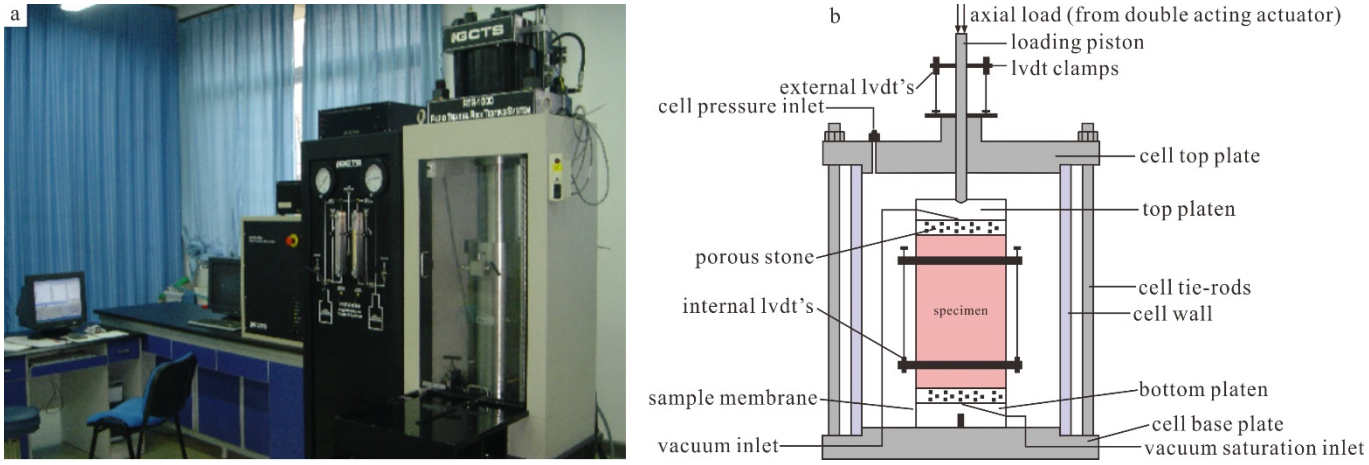

Figure 2. Triaxial stress test system (a) and the structure of the experiment instrument (b).

3.2. X-ray diffraction (XRD) test and petrographic analysis

After completing the systemically triaxial stress test of all rock samples, mineral component of the plunger samples was analyzed by XRD. The analysis procedure was follows: (1) crashing— 1~2 g rock samples was crushed into particles with diameter < 1mm; (2) Milling— sample particles were milled to < 40 μm using a grinder with agate grinding elements in a jar; (3) tablet preparation— the rock powder was placed on an aluminum sample racks on a glass plate, and the sample powder is compressed into tablets; (4) analysis— Mineral composition was analyzed by Bruker D4 Endeavor diffractometer (Bruker Corporation).

The fabric and micromorphological characteristics of rock samples were analyzed by polarized microscope (PM) and scanning electric microscope (SEM). The PM used in this study is an Axio Scope-A1microscope manufactured by Carl Zeiss MicroImaging GmbH. All samples were milled into the thin sections in the thickness of 0.03mm prior to analysis. The SEM used in this study is Quanta 450 FEG manufactured by the FEI Company. The pre-experiment procedure for SEM analysis was as follows: (1) the samples were cleaned with Soxhlet distillation-extraction apparatus and solvent mixtures of chloroform/ methanol for 48 hours; (2) all samples were dried in the oven for 24 hours after cleaning; (3) fresh sections were cut on all sample axes and sprayed with gold evenly.

All the works were processed at the Key Laboratory of Reservoir Description of China National Petroleum Corporation (CNPC).

4. **Results**

4.1. Analytical results

The XRD analytical results show that a total of 8 different minerals were detected in the reservoir rocks in the Upper Member of the Xiaganchaigou Formation, and the mineral compositions of samples are quite different (Table 3). The carbonate minerals (calcite + siderite + dolomite) are the most abundant in the samples 1-44-1, 5-47-1, 12-3-1 and 12-8-1, ranging from 40.00% to 56.60%; anhydrite is the predominant mineral in samples 2-126-1, 4-1-1 and 16-3-1, with a content of 47.30% to 55.50%; and samples 8-27-1, 5-6-1 and 9-36-1 are dominated by clastic and clay minerals. According to the mineral composition of the reservoir, the rock types can be subdivided into three types as carbonate rock, sulphate rock and argillaceous rock.

In addition to the mineral analysis results, the triaxial test results reveal the variation of geomechanical properties among the samples with the mineral composition (Table 3).

Preprints (www.preprints.org) | NOT PEER-REVIEWED | Posted: 24 October 2022 doi:10.20944/preprints202210.0352.v1

As two widely used brittleness parameters (Rickman et al., 2008; Labani and Rezaee, 2015), the Young's Modulus and Poisson's ratio of reservoir rocks in the Upper Member of the Xiaganchaigou Formation range from 21812.50 to 43278.20 MPa and 0.22 to 0.38, respectively. The peak stress or so-called failure limit of samples is 147.31 ~ 361.39 MPa, and the elastic limits is 50% of the peak stress referring the national standard published by the Ministry of Housing and Urban-Rural Development of the People's Republic of China (2013).

Table 3. Mineral composition and triaxial experiment results of samples.

Sample	depth	Q	F	Cal	Sid	Dol	Anh	Py	Clay	Young's Modulus	Elastic limit	Peak Stress	Poisson's ratio
	m	%								MPa			
1-44-1	4078.37	9.70	4.90	9.10	0.90	36.90	38.50	nd.	nd.	43278.20	174.26	348.51	0.34
5-47-1	4122.64	5.70	8.60	8.80	0.80	46.80	14.60	6.10	8.50	37515.00	180.69	361.39	0.27
12-3-1	3860.48	8.20	5.50	19.40	10.80	26.40	16.40	2.10	11.20	37965.80	156.00	311.99	0.36
8-27-1	4146.50	16.70	12.20	6.30	11.00	21.80	2.10	4.70	25.30	33328.90	141.06	282.64	0.35
2-126-1	4096.66	5.60	3.10	nd.	nd.	35.70	55.50	nd.	nd.	37191.00	131.02	262.04	0.38
4-1-1	4106.75	8.20	10.40	7.00	1.60	14.70	55.00	nd.	3.10	35145.70	125.66	251.32	0.22
12-8-1	3861.30	9.20	7.70	12.20	1.20	26.60	29.20	2.00	11.90	32191.70	123.15	246.30	0.37
16-3-1	4202.26	6.10	9.00	nd.	nd.	26.10	47.30	2.60	8.70	32399.10	137.80	275.59	0.38
9-36-1	3794.30	15.70	6.50	0.90	8.00	19.50	13.50	3.80	32.00	23921.70	87.45	174.90	0.22
5-6-1	3766.90	22.70	12.80	17.70	nd.	17.10	4.10	4.40	21.30	21812.50	73.65	147.31	0.27

"nd."- no data; Q-quartz; F-feldspar; Cal-calcite; Sid-siderite; Dol-dolomite; Anh-anhydrite; Py-pyrite.

4.2. Stress-Strain curves

The stress-strain curves of the reservoir rock in the triaxial stress test not only reflect the relationship between stress and strain during compaction and deformation, but also reveal various mechanical properties of the rocks (Meng, et al., 2006; Zhao, et al., 2019). Although many rocks exhibit coupled elastoplastic damage behavior, there are still large difference in mechanical properties between different rocks (Shao et al., 2004). The stress-strain curves of the test samples exhibit different characteristics, and all curves can be subdevided into O, A, B, C, D, E according to their shapes and stress threshhold points (Fig. 4). As described by Zhou et al. (2018) and Xiong et al. (2019) for different stages of stress-strain curves, the crack closure stage (O - A), linear elastic stage (A - B), stable crack growth stage (B - C), unstable crack growth stage (C - D), and the stress relief stage (D - E) after the failure limit point D. All rock samples can be classified into 5 types according to the curve shape and corresponding stress threshold (Fig. 4; Table 3). Type I including samples 5-47-1 and 1-44-1 is characterized by a high failure limit of ~350 MPa and no O—A stage, indicating the natural fractures are not widely developed within the rock samples (Fig. 4a, 4b). The type of stress-strain curve is similar to the failure model for elastic-plastic materials proposed by Vincent (1982). Type II is represented by samples 12-3-1 and 8-27-1 (Fig. 4c, 4d), whose failure limits are much lower (311.9 and 288.64 MPa, respectively). Another distinctive feature of Type II is that the stress-strain curves exhibit a periodic stress drop pattern after the failure limit, indicating that this type of reservoir rock is in a pulse failure mode of plastic materials (Vincent, 1982). The samples of 2-162-1 and 4-1-1 are classified as the Type III, which is characterized by a similar shape to the type I curve but with a much lower failure limit. (Fig. 4e, 4f). The shape of the stress-strain curves of samples 16-3-1, 12-8-1 and 9-36-1 show mixed characteristics of Type I, Type II and Type III, which belong to Type IV. Their curves show elastic-plastic failure features, while the curves in the post-peak region demonstrate very weak impulse failure characteristics (Fig. 4g, 4h ,4i). Sample 5-6-1 represents the fifth type (Type V) with completely different characteristics from other samples (Fig. 4j), which is a typical plastic failure model (Vincent, 1982). The pre-peak region of the Type V curves contains four complete deformation

Preprints (www.preprints.org) | NOT PEER-REVIEWED | Posted: 24 October 2022 doi:10.20944/preprints202210.0352.v1

stages, and the post-peak region show a sharp drop of stress and then a stable stage (Fig. 4j).

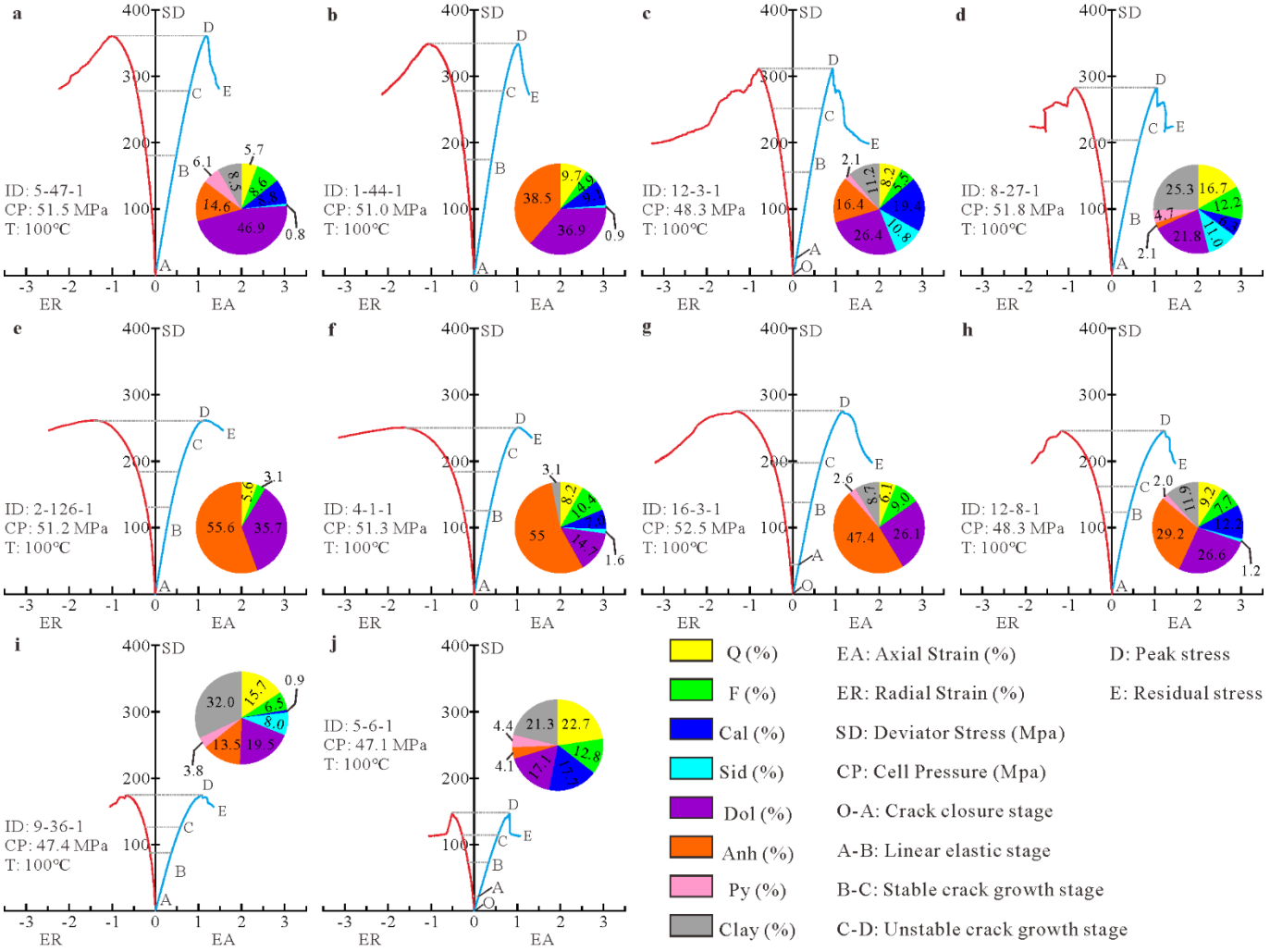

Figure 4. Diagrams of deviator stress-strain curves and the corresponding thresholds of different reservoir rocks (implications of corresponding thresholds after Zhou et al. (2018) and Xiong et al. (2019)).

5. Discussion

Mineral compositions of different rock samples show various trends with stress-strain types (Fig. 4). Brittle rocks with high strength are usually composed of brittle minerals such as quartz, feldspar, and dolomite, etc. Mineral brittleness index (MBI) has been widely used in reservoir evaluation, but its calculation equations is different (Table 4). Quartz, feldspar and carbonate minerals all have positive effects on reservoir brittleness in the equation (Table 4). The brittleness index is related to the content of brittle mineral quartz, carbonate, and pyrite. On the other hand, the ductility index matches the content of ductile minerals such as clay, anhydrite, etc. (Jarvie et al., 2007; Jin et al., 2015; Mathews et al.,2015). The brittle mineral content (Q+F+Cal+Sid +Dol) is the driver of reservoir brittleness (Roger et al., 2011; Glorioso et al., 2012).

According to the stress-strain curves and mineral composition, typeV (Fig. 4j) and typeII (Fig. 4c, 4d) are the most brittle rock types, and their strain curves tend to stabilize after one or more stress drops. However, the steady state after the stress drop suggests that the fracturing effect of the reservoir may not be effective. In addition, the lower content of dolomite in this lithofacies combination reduces matrix porosity results in poor fracturing. Although the brittle mineral content, Young's modulus and failure limit (peak stress) of the 5-47-1, 1-44-1 and 12-3-1 samples are higher, the overal trend correlation

Preprints (www.preprints.org) | NOT PEER-REVIEWED | Posted: 24 October 2022 doi:10.20944/preprints202210.0352.v1

between mechanical indices and the brittle mineral content is not significant (Fig. 4a, 4b ,4c). For example, the 2-126-1 and 4-1-1 samples with higher contents such as clay or anhydrite are considered to be typical plastic minerals (Fig. 4e, 4f ; Zouaoui et al., 2017, Xu et al., 2017) . Therefore, the MBI equation widely used in shale reservoir brittleness evaluation is not necessarily fully applicable to continental fine-grained sedimentary rock reservoirs. To clarify the contribution of different minerals to reservoir brittleness, the correlation between mineral facies and mechanical properties needs to be analyzed. In addition, the occurrence state and particle size of minerals in reservoir rocks are also key factors affecting the mechanical properties of the rocks (Hudson and Harrison, 1997).

Table 4. MBI calculation equations.

Correlation for MBI	Formation	Lithology	Φ/%	TOC/%	Reference
$\frac{Q}{Q+Carb+Clay}$	Barnett	Shale bounded by limestone	6	1-3	Jarvie et al., 2007
$\frac{Q+Dol}{Q+Dol+Cal+Clay+TOC}$	Barnett	Shale bounded by limestone	6	1-3	Wang and Gale, 2009
$\frac{Q+Cal+Dol}{Q+Cal+Dol+Clay+TOC}$	Neuquén Basin, Argentina	Mudstones	8	2.5-3.5	Glorioso and Rattia, 2012
$\frac{Q+F+M+Carb}{tot}$	Barnett	Shale bounded by limestone	6	1-3	Jin et al., 2014

Carb-carbonate, M-mica; TOC-total organic carbon; tot- total weight fraction.

5.2. Correlation between mineral and mechanical properties

Brittle minerals are the main controlling factor for rock brittleness, while ductile minerals are the opposite (Jarvie et al., 2007; Jin et al., 2014). The natural properties of minerals indicate that brittle minerals have higher hardness (Table 5). The most ideal brittle minerals are quartz and feldspar, followed by carbonate minerals (dolomite and calcite), while sulfate minerals and clay minerals (harder than talc) are not conductive to the rock brittleness. Under this assumption, the mineral content of quartz and feldspar in brittle reservoir should be relatively higher. However, the stress-strain curve in Fig. 4 shows that the mechanical properties of mixed fine-grained sedimentary rocks in the study area are more complicated than assumed. Figure 5 shows the binary fitting results of different minerals and mechanical properties of reservoir rocks.

Table 5. Mineralogical information of common rock-forming minerals.

Mineral	Chemical formula	Crystal system	Cleavage	Mohs Hardness	Microhardness /GPa	Reference
talc	$Mg_3Si_4O_{10}(OH)_2$	monoclinic	perfect{001}	1	0.14 ± 0.03	Broz et al., 2006
gypsum	$CaSO_4{\cdot}2H_2O$	monoclinic	perfect{010}, good{100}	2	0.61 ± 0.15	
anhydrite	$CaSO_4$	orthorhombic	perfect{010}, good{001}	2~3	1.32±0.13	Brace, 1960
calcite	$CaCO_3$	trigonal	perfect{1010}	3	1.49 ± 0.11	Broz et al., 2006
dolomite	$CaMg(CO_3)2$	trigonal	Perfect{1011}, Perfect{1011}	3.5~4	3.35±0.33	Wong and Bradt, 1992
orthoclase	$KAlSi_3O_8$	monoclinic	perfect{001},good{010}	6	6.87 ± 0.66	Broz et al., 2006
quartz	SiO_2	trigonal	none	7	12.2 ± 0.61	

The comparison results of X-ray diffraction and triaxial stress tests revealed that the content of dolomite was positively correlated with Young's modulus and peak stress, with fitting ratios(r^2) of 0.69 and 0.57, respectively (Fig. 5 a-c). The results further exhibit that the stiffness and strength of the reservoir rock are positively related with the dolomite content. The intersection curve of dolomite content and Poisson's ratio is characterized by an upward concave (r^2=0.79). When the dolomite content is greater than ~30%, the Poisson's ratio is significantly negatively correlated with dolomite content (Fig. 5 b), wihle the

 doi:10.20944/preprints202210.0352.v1

Poisson's ratio decreases with the increase of Young's modulus. According to the criteria proposed by Rickman et al. (2008) and Labani and Rezaee (2015), this type of reservoir rock sample is a typical representative of brittle reservoir rock.

On the other hand, the quartz and feldspar, two brittle minerals widely considered to be high hardness (Jarvie et al., 2007; Jin et al., 2014) were negatively correlated with Young's modulus and peak stress, respectively(Fig 5d, f, Table 5). Poisson's ratio shows a very weak negative correlation with the content of quartz and feldspar, indicating that the content of quartz and feldspar in mixed fine-grained sedimentary rocks with mixed characteristics contributes little to rock brittleness. These phenomena are inconsistent with the prevailing view of the relationship between rock mechanical properties and mineral composition, suggesting that the total content of brittle minerals may not be the only driver of the brittleness of the reservoir rocks in the study area. It is often reported that petrographic properties affect mechanical properties (Räisänen, 2004; Abbas et al., 2018). Therefore, the controlling effect of rock internal structure and texture on rock mechanical properties needs to be further explored.

The low correlation between anhydrite content and mechanical properties suggests that this type of mineral has little effect on rock brittleness(figure 5 g-i). The clay mineral content has a negative binary correlation with the mechanical properties (Fig. 5 j-l), indicating that reservoir brittleness is compromised with increasing clay content. It is well known that the clay content in typical shale oil reservoirs contributes more to brittleness (reference). The brittleness and ducility characteristics of samples with high clay content mainly depend on the way their particle are supported. The special contact relationship between clay particles can effectively enhance the ducility of rock skeleton, while the stratified structure of clay in shale can reduce the static Poisson ratio of rock skeleton.

To sum up, the content of dolomite and clay showed a correlation with mechanical properties, which is consistent with the general opinion. Mineral composition is not a simple controlling factor of rock mechanical properties, and analysis of rock petrographic characteristics (such as fabric) may be a necessary conditon to understand the controlling factors of rock brittleness.

Preprints (www.preprints.org) | NOT PEER-REVIEWED | Posted: 24 October 2022 doi:10.20944/preprints202210.0352.v1

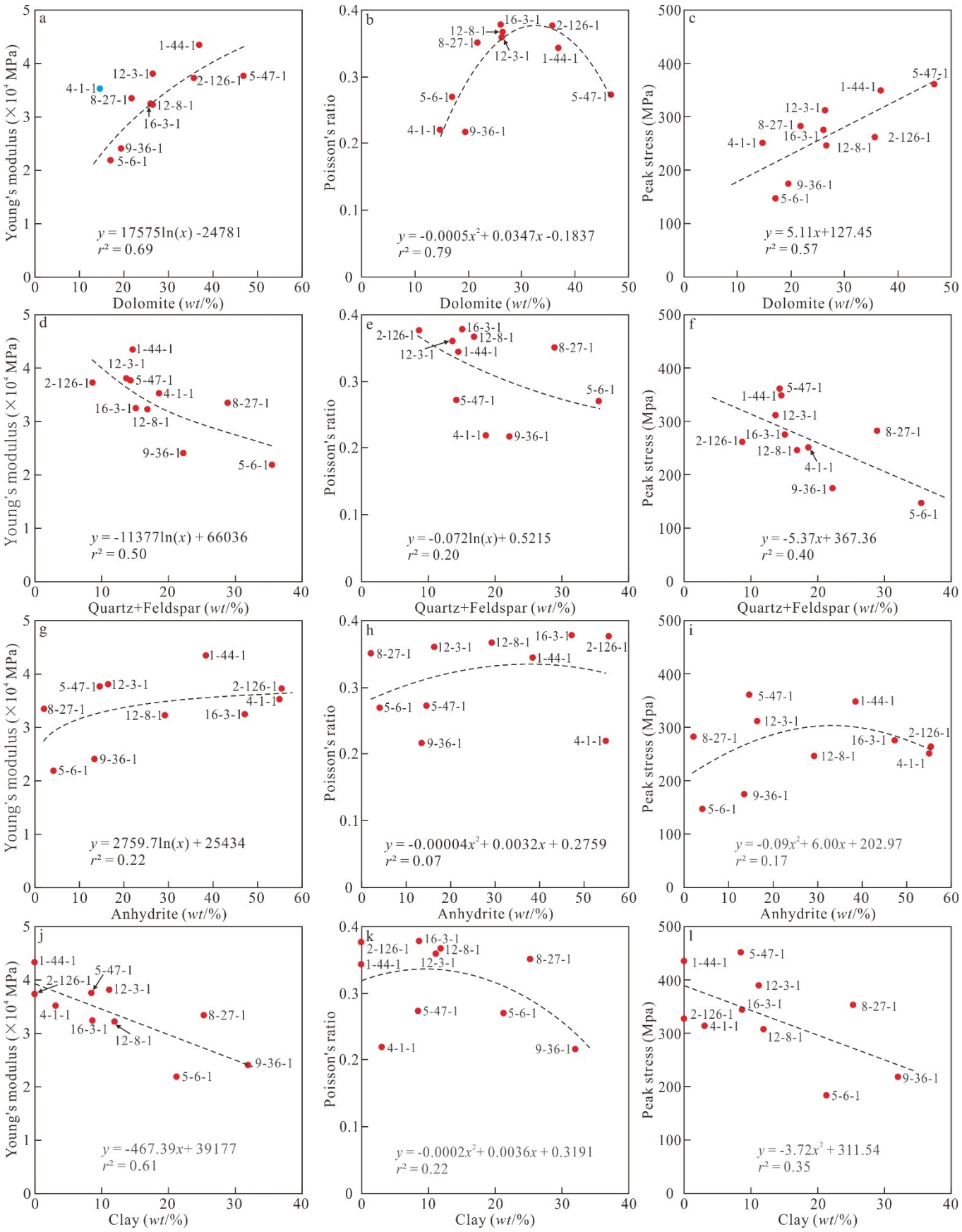

Figure 5. Correlations between mineral content and mechanical properties (The blue point does not participate in the fitting).

5.3. Petrography impact on mechanical property

Preprints (www.preprints.org) | NOT PEER-REVIEWED | Posted: 24 October 2022 doi:10.20944/preprints202210.0352.v1

Since the depositional environment of the studied strata was the depositional center of the saline lake and had undergone continuous late intense tectonic deformation (Zhang et al., 2018), the reservoir morphologies are dominated by massive, bedded and laminated features. In order to understand the impact of petrography on the mechanical properties of samples, polarized microscopy (PM) and scanning electronic microscopy (SEM) were used to systemically analyze the structure and texture of rocks. Rock samples with different morphologies show different mechanical properties, which are mainly controlled by the grain characteristics and combinations forming the rock skeleton.

The images of PM and SEM show that the rock skeleton is mainly composed of a microcrystalline structures dominated by dolomite particles. The high-hardness framework (Table 5) composed of microcrystalline dolomite structure generally presents higher pressure-bearing capacity and better brittleness, while other minerals scattered in rocks contribute less to the rock strength. On the other hand, the high strength of the rock preserves a large number of dolomite intercrystalline pores, which lays the foundation for the good storage capacity and fracturing stimulation capacity of this type of reservoir. There are 8 test samples with porphyritic texture in the test, accounting for 80% of the total. These porphyritic samples were composed of different fabrics, resulting in significant differences in mechanical properties.

According to the stress-strain curves in Fig. 4, different rock samples were classified into 5 categores. Among them, Type I samples (5-47-1 and 1-44-1) show the best brittleness properties with massive structure and porphyritic texture (Fig. 6a, b). The structural feature of Type I is similar to the anhydrite-rich samples, but with a different matrix texture. The Type II samples of 12-3-1 and 8-27-1 are in structures of bedded and massive and are in textures of porphyritic and sandy-micritic, respectively (Fig. 6c, d). The stress-strain curve of sample 12-3-1 in Type I (Fig. 4c) shows a crack closure stage (O—A), which does not exist in curves of 5-47-1, 1-44-1 and 8-27-1 in Type II (Fig. 4a, b, d). This phenomenon is caused by the interbedded cracks revealed in the microscopic images in Fig. 6c. The microscopic images of sample 8-27-1 reveal numerous scattered or bedded terrigenous silt grains (Fig. 6d). The clay mineral content in Type II samples is significantly higher than that in Type I samples, indicating that the increase in the proportion of clay mineral is one of the reasons for plastic deformation of samples. In addition, petrographical interfaces usually undergo sliding deformation after peak stress, such as the bedding plane of sample 12-3-1 and the contact interface of the silt and micrite of sample 8-27-1 (Fig. 6d). These petrographical interfaces exhibit plastic deformation characteristics, which are weak interfaces. Furthermore, Type II samples exhibit plastic deformation characteristics but exhibit strength limit second only to Type I, which may be related to their low porosity. In fact, the negative effect of the porosity of rocks on their strength has been investigated in previous studies (Palchik and Hatzor, 2004).

Based on the similar dolomitic skeleton, the Type III samples (2-162-1 and 4-1-1) have similar petrographical characteristics to the Type I samples(Fig. 6e, f). The difference in stress strength between the two types may be caused by the anhydrite proportion, among which the content of softer anhydrite in Type III is much higher than that of Type I (Fig. 6e, f).

The samples of 16-3-1, 12-8-1 and 9-36-1 are classified as the Type IV according to the stress-strain curve shapes, which shows mixed characteristics of Type I, Type II and Type III (Fig. 3). This phenomenon was caused by the combination of mineral composition and rock fabrics. The mineral composition of Type IV varies widely, among which the lower clay minerals of the 16-3-1 and 12-8-1 samples determine their brittleness better than the 9-36-1 sample (Fig. 3, Table 3). Furthermore, the petrographic characteristics of these samples are also different, samples of 16-3-1 and 12-8-1 present massive structure and porphyritic texture (Fig. 6g, h). Although some fine-grained terrigenous detritus and clays are present, a higher proportion of dolomite particles can still form the rock skeleton, resulting in a strength limit similar to that of type III. The high proportion of clay minerals in the 9-36-1 sample cannot form a solid framework except for the layered structure (Fig. 6i), showing strong ductility.

Preprints (www.preprints.org) | NOT PEER-REVIEWED | Posted: 24 October 2022 doi:10.20944/preprints202210.0352.v1

The sample of 5-6-1 belong to the Type V, which is characterized by laminated structure and muddy texture (Fig. 6i). The higher content of clay minerals and laminated petrographic characteristics are favorable for the development of many weak interfaces in the rock, contributing to a significant ductile deformation characteristic under the compressional conditions.

In summary, the samples with massive structure and dolomite matrix skeleton are more brittle than the samples with layered structure (bedded and laminated) and lack of dolomite skeleton.

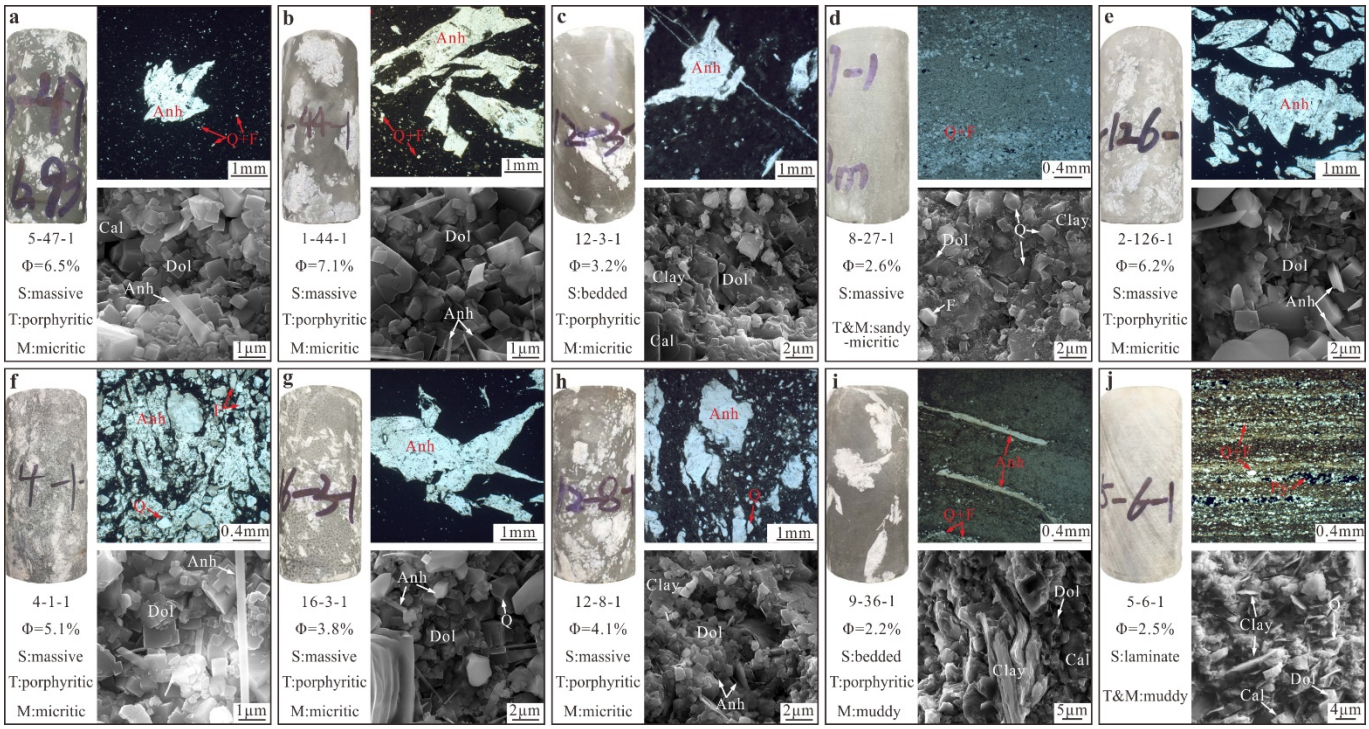

Figure 6. Petrographical charateristics of tested samples (Φ-porosity, S-structure, T-Texture, M-texture of matrix).

5.4. Standard of reservoir brittleness classification and practical effect

The discussion of different rock brittleness and controlling factors of the reservoir revealed that mineral composition and heterogeneity are of great significance to the evaluation of reservoir geomechanical characteristics and stimulation potential. Therefore, based on the results of the triaxial compression experiments and the petrographic analyses, a comprehensive local standard of reservoir brittleness classification has been suggested to guide stimulation engineering (Table 6). The standard classifies the reservoir rocks in the study area into three grades: good, medium and poor. Brittle oil reservoirs are usually characterized by high Young's modulus and low Poisson's ratio, which are negatively correlated (Rickman et al., 2008; Labani and Rezaee, 2015). The correlation between mineral composition and mechanical properties reveals that when the proportion of the dolomite is higher than ~30%, Young's modulus demonstrates a negative correlation with Poisson's ratio (Fig. 5b), indicating the brittle reservoirs. Combined with petrographic characteristics, the high-content dolomite, low-content clay, massive structure and dolomite skeleton constitute good reservoirs. Considering the storage capacity of hydrocarbon and the impact of the pores on rock mechanics, the porosity of this type of reservoir is usually greater than 6%. The other two grades (medium and poor) of reservoir brittleness evaluation criteria are also defined in Table 6, including parameters such as mineral content, petrology, mechanical properties and porosity. All the tested

Preprints (www.preprints.org) | NOT PEER-REVIEWED | Posted: 24 October 2022 doi:10.20944/preprints202210.0352.v1

samples are divided into 3 groups, according to the present standard, including the good samples of 1-44-1, 5-47-1 and 2-126-1, medium samples of 12-3-1, 12-8-1 and 16-3-1, and poor samples of 8-27-1, 2-126-1, 4-1-1, 9-36-1 and 5-6-1.

Table 6. Local standard of reservoir brittleness classification.

Grade	Mineral composition (%)		Petrography		Mechanics (MPa)		Porosity (%)
	dolomite	clay	structure	skeleton texture	Young's modulus	peak stress	
good	> 30	< 10	massive	micritic	> 37000	> 260	≥6.0
medium	20~30	< 20	massive/bedded	micritic	> 32000	> 240	≥3.5
poor	< 20	< 40	massive/bedded/laminated	argillaceous	> 20000	> 140	≥1.0

In order to prove the rationality of the standard, the stimulation effect and brittleness characteristics of heterogeneous reservoirs in the study area were revealed through lithology model and microseismic monitoring results of horizontal well volume fracturing (Fig. 7). Warmer colors in the lithology model mean higher dolomite content and better brittleness (Fig. 7). In practice applications, the density and intensity of micro-seismic events are usually recognized as an indicator of the fracturability of the reservoir. In practical applications, microseismic detection is used to record the density and intensity of seismic events after single-well hydraulic fracturing, representing the occurrence of brittle reservoir stimulation. The micro-seismic events and lithology model of reservoirs show a good spatial correlation (Fig.7 b, c). The fracturing stages 1, 2, 5, 6, 7 (Fig.7 b, c, f) triggered more and stronger micro-seismic events than that of the stages of 3 and 4, which is in accordance with the distribution of the dolomite. The consistent result of brittleness and reservoir stimulation provides a good practical case for studying the impact of lithologic heterogeneity on reservoir brittleness.

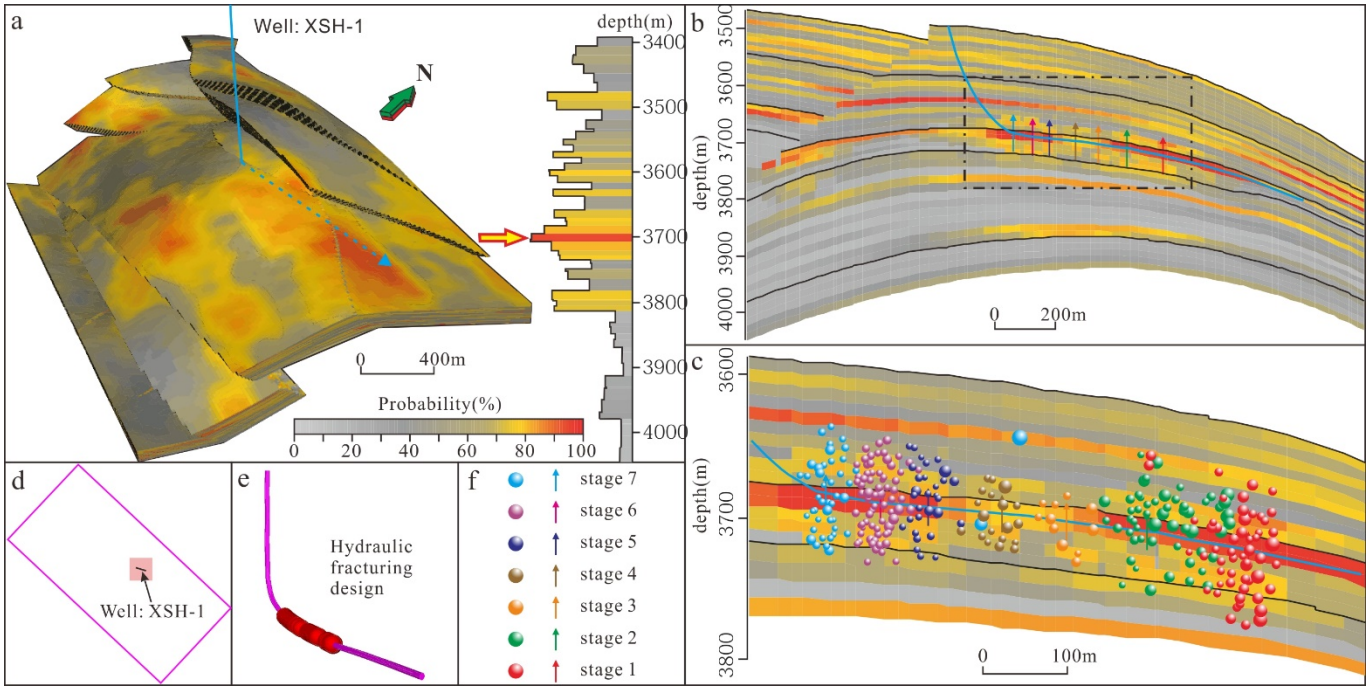

Figure 7. The micro-seismic monitoring data and lithology probability model of a stimulated horizontal well. (a- the 3D probability model of the good reservoir distribution; b- profile of the probability model; c- micro seismic event points of the hydraulic fracture, c is the enlargement of the dash line box in b; d- well location; e- well trajectory and hydraulic fracturing design; f- the colored balls and arrows indicate the micro seismic event and fracturing location of each stage, the size of the ball indicates the strength of the seismic event.).

 doi:10.20944/preprints202210.0352.v1

6. Conclusion

After a comprehensive discussion of the triaxial compression experiment and the petrography of the reservoir rocks in the Upper Member of the Xiaganchaigou Formation in the western Qaidam basin, knowledge of the mechanical properties and their controlling factors of tight-mixed carbonate reservoirs are concluded as follows:

(1) The shape of stress-strain curves and the corresponding stress thresholds suggest that the tested samples can be subdivided into 5 types with different mechanical properties. The stress-strain curve characteristics of the type I specimen and the type III specimen are both elastoplastic failure modes, but the failure limit of the type I specimen is higher than that of the type III specimen. The samples of Type II show a special pulse failure mode of the plastic material. The stress failure mode of Type IV samples shows the mixed characteristics of Type I, Type II, and Type III, although their failure limit varies significantly. However, Type V shows a typical plastic failure model.

(2) The correlation between minerals and mechanical properties indicate that the widely used MBI equations is not completely applicable to the studied stratum. The commonly recognized brittle minerals such as quartz and feldspar have no obvious positive correlation with the mechanical properties which characterize the brittleness in tight mixed carbonate. The dolomite and clay minerals show good positive and negative correlations with the mechanical properties of brittleness respectively in tight mixed carbonate. The continuous deformation after the peak and the dolomite skeleton with developed intercrystalline pores are the main indicators of the brittleness and effectiveness of tight mixed carbonate rocks.

(3) The result of petrographic analysis proves the contribution of dolomite to rock brittleness, and confirms that dolomite particles constitute the rock skeleton of tight mixed carbonate brittle reservoir. In addition, the high hardness of the dolomite skeleton preserve a mount of intercrystalline pores while resisting high compressive stress, thus playing a positive role in hydrocarbon preservation. Lithofacies with lower dolomite content is difficult to form a strong rock skeleton, so its brittleness and storage capacity are relatively low.

(4) Based on the understanding of the research strata, a set of brittleness evaluation standards for tight mixed carbonate rocks was determined, and the validity of the standards was verified by the spatial correlation between the stimulated horizontal well microseismic monitoring data and lithology probability models.

Acknowledgment: This work was supported by National Natural Science Foundation of China (Grant No. 51709127).

Reference

1. Abbas, A.K., Flori, R.E., Alsaba, M., 2018. Estimating rock mechanical properties of the Zubair shale formation using a sonic wireline log and core analysis. Journal of Natural Gas Science and Engineering, 53, 359-369.
2. Aderibigbe, A., Valdes, C. C., Heidari, Z., 2016. Integrated rock classification in the Wolfcamp Shale based on reservoir quality and anisotropic stress profile estimated from well logs. Interpretation, 4 (2), SF1-SF18.
3. Åkesson, U., Stigh, J., Lindqvist, J. E., & Göransson, M., 2003. The influence of foliation on the fragility of granitic rocks, image analysis and quantitative microscopy. Engineering Geology, 68(3-4), 275-288.
4. Bishop, A. W., 1967. Progressive failure with special reference to the mechanism causing it: In Proc. Geotech. Conf., Oslo, 2, 142–150.
5. Bodziak, R., Clemons, K., Stephens, A., Meek, R., 2014. The role of seismic attributes in understanding the hydraulically fracturable limits and reservoir performance in shale reservoirs: An example from the Eagle Ford Shale, south Texas. AAPG Bull., 98 (11): 2217-2235.
6. Bodziak, R., Clemons, K., Stephens, A., Meek, R., 2014. The role of seismic attributes in understanding the hydraulically fracturable limits and reservoir performance in shale reservoirs: An example from the Eagle Ford Shale, south Texas. AAPG Bull., 98 (11): 2217-2235.
7. Brace, W.F., 1960. Behavior of Rock Salt, Limestone, and Anhydrite during Indentation. Journal of Geophysics Research, 65(6), 1773-1788.

8. Broz, M.E., Cook, R.F., Whitney, D.L., 2006. Microhardness, toughness, and modulus of Mohs scale minerals. American Mineralogist, 91, 135–142.
9. Buller, D., Hughes, S. N., Market, J., Petre, J. E., Spain, D. R., and Odumosu, T., 2010. Petrophysical evaluation for enhancing hydraulic stimulation in horizontal shale gas wells: In SPE Annual Technical Conference and Exhibition Society of Petroleum Engineers.
10. Bustin, A.M. M., and R. M. Bustin, 2012. Importance of rock properties on the producibility of gas shales: International Journal of Coal Geology, v. 103, p. 132–147.
11. Curtis, J.B., 2002. Fractured shale-gas systems, AAPG Bull. 86 (11), 1921–1938.
12. Deng, Y., Pu, X. G., Chen, S. Y., Yan, J. H., Shi, Z. N., Zhang, W., & Han, W. Z., 2019. Characteristics and controlling factors of fine-grained mixed sedimentary rocks reservoir: A case study of the 2nd member of Kongdian formation in Cangdong depression, Bohai Bay basin. Journal of China University of Mining and Technology, 48(6), 1301-1316.
13. Donath, F. A., 1970. Some information squeezed out of rock: American Scientist, v. 58, p. 54–72.
14. Dong, T., Harris, N. B., Ayranci, K., Yang, S., 2017. The impact of rock composition on geomechanical properties of a shale formation: Middle and Upper Devonian Horn River Group shale, Northeast British Columbia, Canada. AAPG Bulletin, 101(2): 177-204.
15. EIA, 2013. Technically recoverable shale oil and shale gas resources: an assessment of 137 shale formations in 41 countries outside the United States, pp. 1-150.
16. Ersoy A., Waller M. D., 1995. Textural characterization of rocks. Engineering Geology, 39 (3/4): 123-136.
17. Fairbanks, M.D., Ruppel, S.C., Rowe, H., 2016. High-resolution stratigraphy and facies architecture of the Upper Cretaceous (Cenomanian-Turonian) Eagle Ford Group, Central Texas. AAPG Bull. 3, 379–403.
18. Ferrill, D. A., and A. P. Morris, 2008. Fault zone deformation controlled by carbonate mechanical stratigraphy, Balcones fault system, Texas: AAPG Bulletin, v. 92, p. 359–380.
19. Fu, S., Ma, D., Chen, Y., Zhang, G., Wu, K., 2016. New advance of petroleum and gas exploration in Qaidam Basin. Acta Petrolei Sinica, 37(S1), 1-10.
20. Ge, X. R., 1997, Post failure behavior and a brittleplastic model of brittle rock: Computer Methods and Advances in Geomechanics, 151-160.
21. Geng, Z., Chen, M., Jin, Y., Yang, S., Yi, Z.C., Fang, X., Du, X.Y., 2016. Experimental study of brittleness anisotropy of shale in triaxial compression. J. Nat. Gas Sci. Eng. 36, 510-518.
22. Glorioso, J. C., & Rattia, A., 2012. Unconventional reservoirs: basic petrophysical concepts for shale gas. In SPE/EAGE European unconventional resources conference & exhibition-from potential to production (pp. cp-285). European Association of Geoscientists & Engineers.
23. Glorioso, J.C., Rattia, A., 2012. Unconventional Reservoirs: Basic Petrophysical Concepts for Shale Gas. In Proceedings of the SPE/EAGE European Unconventional Resources Conference and Exhibition from Potential to Production, Vienna, Austria, SPE-153004-MS.
24. Goodway, B., Varsek, J., Abaco, C., 2006. Practical applications of P-wave AVO for unconventional gas Resource Plays. CSEG Recorder, 31, 52-65.
25. Heidari, M., Khanlari, G. R., and Torabi, K. M., 2014. Effect of Porosity on Rock Brittleness: Rock Mechanics and Rock Engineering, 47(2), 785-790.
26. Hentz, T.F., Ambrose, W.A., Smith, D.C., 2013. Eaglebine play of the southwestern East Texas basin: stratigraphic and depositional framework of the Upper Cretaceous (Cenomanian-Turonian) Woodbine and Eagle Ford Groups. AAPG Bull. 12, 2551-2580.
27. Hucka, V., and Das, B., 1974. Brittleness determination of rocks by different methods: International Journal of Rock Mechanics and Mining Sciences and Geomechanics Abstracts, 11(10), 389-392.
28. Hudson, J.A, Harrison J P, 1997. Engineering rock mechanics, Part 1: an introduction to the principles. Oxford: Elservier Ltd, pp 429.
29. Jarvie, D.M., Hill, R.J., Ruble, T.E., Pollastro, R.M., 2007. Unconventional shale-gas systems: the Mississippian Barnett Shale of north-central Texas as one model for thermogenic shale-gas assessment. AAPG Bull. 91, 475-499.
30. Jarvie, D.M., Hill, R.J., Ruble, T.E., Pollastro, R.M., 2007. Unconventional shale-gas systems: the Mississippian Barnett Shale of north-central Texas as one model for thermogenic shale-gas assessment. AAPG Bull. 91, 475-499.
31. Jin, X., Shah, S.N., Roegiers, J.C., Zhang, B., 2015. An integrated petrophysics and geomechanics approach for fracability evaluation in shale reservoirs. Soc. Pet. Eng. J. 20 (3), 518-526.
32. Jin, X.; Shah, S.N.; Roegiers, J.C.; Zhang, B., 2014. Fracability Evaluation in Shale Reservoirs—An Integrated Petrophysics and Geomechanics Approach. In Proceeding of the SPE Hydraulic Fracturing Technology Conference, The Woodlands, Texas, USA, SPE-168589-MS.
33. Kuang L. C., Hou L. H., Yang Z., Wu, S., 2021. Key parameters and methods of lacustrine shale oil reservoir characterization. Acta Petrolei Sinica, 2021, 42 (1): 1-14.
34. Kuhn, P.P., Primio, R.D., Hill, R., Lawrence, J.R., Horsfield, B., 2012. Three-dimensional modeling study of the low-permeability petroleum system of the Bakken Formation. AAPG Bull. 10, 1867-1897.

35. Labani, M.M., Rezaee, R., 2015. The importance of geochemical parameters and shale composition on rock mechanical properties of gas shale reservoirs: a case study from the Kockatea shale and Carynginia formation from the Perth basin, Western Australia. Rock Mech. Rock Eng. 48, 1249-1257.
36. LI Maowen, MA Xiaoxiao, JIANG Qigui, et al. Enlightenment from formation conditions and enrichment characteristics of marine shale oil in North America. Petroleum Geology and Recovery Efficiency, 2019, 26(1): 13-28.
37. Li, L., Wang, Z. X., Zheng, Y. H., Chen, F. L., Wu, S. Q., Qi, Z. X., & Liu, A. W. (2019). Mechanism of shale oil enrichment from the salt cyclotherm in Qian3 Member of Qianjiang sag, Jianghan Basin. Earth Science, 44(3), 1012-1023.
38. Li, Z., Li, L., Li, M., Zhang, L., Zhang, Z., Huang, B., Tang, C., 2018. A numerical investigation on the effects of rock brittleness on the hydraulic fractures in the shale reservoir. J. Nat. Gas Sci. Eng. 50, 22-32.
39. Lu, H., Xiong, S., 2009. Magnetostratigraphy of the Dahonggou section, northern Qaidam Basin and its bearing on Cenozoic tectonic evolution of the Qilian Shan and Altyn Tagh Fault. Earth and Planetary Science Letters, 288(3-4): 539-550.
40. Maowen, L. I., Xiaoxiao, M. A., Qigui, J. I. A. N. G., Zhiming, L., Xiongqi, P., & Caitong, Z., 2019. Enlightenment from formation conditions and enrichment characteristics of marine shale oil in North America. Petroleum Geology and Recovery Efficiency, 26(1), 13-28.
41. Mathews H L, Schein G, Malone M. Stimulation of gas shales: they' re all the same-right?. SPE Hydraulic Fracturing Technology Conference, 2007: 29-31.
42. Meng, Z., Zhang, J., Peng, S., 2006. Influence of sedimentary environments on mechanical properties of clastic rocks. Environmental Geology, 51, 113–120.
43. Mews, K.S, Alhubail, M.M, Barati, R.G, 2019. A review of brittleness index correlations for unconventional tight and ultra-tight reservoirs. Geosciences, 9, 319.
44. Ministry of Housing and Urban-Rural Development of the People's Republic of China, 2013. Standard for test methods of engineering rock mass (GB/T 50266-2013). Beijing: China Planning Press, pp91.
45. Montgomery, S. L., 1996. Permian "Wolfcamp" limestone reservoirs; Powell Ranch Field, eastern Midland Basin. AAPG Bull. 80 (9), 1349-1365.
46. Montgomery, S.L., Jarvie, D.M., Bowker, K.A., Pollastro, R.M., 2005. Mississippian Barnett shale, Fort Worth basin, north-central Texas: gas-shale play with multi-trillion cubic foot potential, AAPG Bull. 89 (2), 155-175.
47. Mullen, M.J., Roundtree, R., Turk, G.A., 2007. A composite determination of mechanical rock properties for stimulation design (what to do when you don't have a sonic log). In: SPE Rocky Mountain Oil & Gas Technology Symposium. SPE-108139-MS
48. Palchik, V., & Hatzor, Y. H., 2004. The influence of porosity on tensile and compressive strength of porous chalks. Rock Mechanics and Rock Engineering, 37(4), 331-341.
49. Paul, S., and Sun, C. C., 2017. Lubrication with magnesium stearate increases tablet brittleness: Powder Technology, 309, 126-132.
50. Räisänen, M., 2004. Relationships between texture and mechanical properties of hybrid rocks from the Jaala–Iitti complex, southeastern Finland. Engineering Geology, 74(3-4), 197-211.
51. Rickman, R., M. Mullen, E. Petre, B. Grieser, and D. Kundert, 2008. A practical use of shale petrophysics for stimulation optimization: All shale plays are not clones of the Barnett Shale: 2008 SPE Annual Technical Conference and Exhibition, Denver, September 21-24, 2008, SPE Paper 115258, 11 p.
52. Rickman, R., Mullen, M.J., Petre, J.E., Grieser, W.V., Kundert, D., 2008. A practical use of shale petrophysics for stimulation design optimization: all shale plays are not clones of the Barnett Shale. In: SPE Annual Technical Conference and Exhibition. SPE-115258.
53. Shao, J. F., Jia, Y., Kondo, D., 2004. An Elastoplastic Damage Model for Unsaturated Argillites. Elsevier Geo-Engineering Book Series, 495-500.
54. Shi, G. C., Ge, X. R., and Lu, Y. D., 2006. Experimental study on coeffi cients of brittle stress drop of marble: Chinese Journal of Rock Mechanics and Engineering, 25 (8), 1625-1631.
55. Slatt R M., 2011. Important geological properties of unconventional resource shales. Central European Journal of Geosciences, 3(4): 435-448.
56. Slatt, R. M., 2011. Important geological properties of unconventional resource shales. Central European Journal of Geosciences, 3(4), 435-448.
57. Sone, H., Zoback, M. D., 2013. Mechanical properties of shale-gas reservoir rocks-Part 1: Static and dynamic elastic properties and anisotropy. Geophysics 78, D381-D392.
58. Sonnenberg, A.S., Pramudito, A., 2009. Petroleum geology of the giant Elm Coulee field, Williston Basin. AAPG Bull. 9, 1127-1153.
59. Tan, W. H., Ba, J., Guo, M. Q., Li, H., Zhang, L., Yu, T., & Chen, H., 2018. Brittleness characteristics of tight oil siltstones. Applied Geophysics, 15 (2), 175-187.
60. Tarasov, B., and Potvin, Y., 2013. Universal criteria for rock brittleness estimation under triaxial compression: International Journal of Rock Mechanics and Mining Sciences, 59 (4), 57-69.
61. Torres-Verdín, C., Victoria, M., Merletti, G., & Pendrel, J. (1999). Trace-based and geostatistical inversion of 3-D seismic data for thin-sand delineation: An application in San Jorge Basin, Argentina. The Leading Edge, 18 (9), 1070-1077.

62. Tyson, R. V., & Pearson, T. H., 1991. Modern and ancient continental shelf anoxia: an overview. Geological Society, London, Special Publications, 58(1), 1-24.
63. Vincent, J.F.V., 1982. Structural biomaterials. London: The Macmillan Press, pp 207.
64. Wang, F.P., Gale, J.F.W., 2009.Screening Criteria for Shale-Gas Systems; Gulf Goast Assoc. Geol. Soc. Trans., 59, 779–793.
65. Wang, J.G., Zhang, D.W., Yang, S.Y., Li, X., Shi, Y.J., Cui, J., Zhang, P., Wang, Y.L., Yi, D.H., Chang, H.Y., 2020. Sedimentary characteristics and genesis of the salt lake with the upper member of the Lower Ganchaigou Formation from Yingxi sag, Qaidam basin. Marine and Petroleum Geology, 111, 135-155.
66. Wong, T.Y., Bradt R.C., 1992. Microhardness anisotropy of single crystals of calcite, dolomite and magnesite on their cleavage planes. Materials Chemistry and Physics, 30, 261-266.
67. Xiong, L., Wu, S., Zhang S., 2019. Mechanical Behavior of a Granite from Wuyi Mountain: Insights from Strain-Based Approaches. Rock Mechanics and Rock Engineering, 52:719–736. https://doi.org/10.1007/s00603-018-1617-8
68. Xu, L., Gao, H., Xu, J., Xu, M., Wang, X., You, F., Long, Y., 2017. Experimental insights into a novel over-saturated brine cement slurry used in anhydrite formation. Bulgarian Chemical Communications, 49, Special Edition K1, 214-219.
69. Yergin, D., 2011. The Quest: Energy, Security, and the Remaining of the Modern World. Penguin Press, London, pp. 1-300.
70. Zhang, Sh. Cao, Y.C., Zhu, R. K, Xi, K. L., Wang, J., Zhu, N., Hu, R.N., 2018. Lithofacies classification of fine grained mixed sedimentary rocks in the Permian Lucaogou Formation, Jimsar sag, Junggar Basin. Earth Science Frontiers, 25(4), 198.
71. Zhang, Y., Wu, K., Jiang, Y., Wang, P., Cai, Z., Gao, F., Tan, W., Gao, S., 2018. Geological Characteristics of Deep Carbonate Hydrocarbon -bearing Pool in the Western Yingxiongling Area in Qaidam Basin. Natural Gas Geoscience, 29(3), 358-369.
72. Zhao, Y., Zhou, H., Zhong, J., Liu, D., 2019. Study on the relation between damage and permeability of sandstone at depth under cyclic loading. International Journal of Coal Science & Technology, 6(4), 479-492.
73. Zhou, L.H., Chen, C.W., Han, G.M., et al., 2019. Geological Characteristics and Shale Oil Exploration Potential of Lower First Member of Shahejie Formation in Qikou Sag, Bohai Bay Basin. Earth Science, 44(8): 2736-2750 (in Chinese with English abstract).
74. Zhou, L.H., Han, G.M., Ma, J.Y., et al., 2020. Palaeoenvironment Characteristics and Sedimentary Model of the Lower Submember of Member 1 of Shahejie Formation in the Southwestern Margin of Qikou Sag. Acta Petrolei Sinica, 41(8): 903-917 (in Chinese with English abstract).
75. Zhou, L.H., Pu, X.G., Chen, C.W., et al., 2018. Concept, Characteristics and Prospecting Significance of FineGrained Sedimentary Oil Gas in Terrestrial Lake Basin: A Case from the Second Member of Paleogene Kongdian Formation of Cangdong Sag, Bohai Bay Basin. Earth Science, 43(10): 3625-3639 (in Chinese with English abstract).
76. Zhou, S., Xia, C., Zhou, Y., 2018. A theoretical approach to quantify the effect of random cracks on rock deformation in uniaxial compression. Journal of Geophysics and Engineering, 15(3), 627–637. doi:10.1088/1742-2140/aaa1ad
77. Zou, C. N., Zhang, G. S., Yang, Z., Tao, S. Z., Hou, L. H., Zhu, R. K., ... & Wang, Z. P., 2013. Geological concepts, characteristics, resource potential and key techniques of unconventional hydrocarbon: On unconventional petroleum geology. Petroleum Exploration and Development, 40 (4), 385-399.
78. Zouaoui, H., Lecomte-Nana, G.L., Krichen, M., Bouaziz, J., 2017. Structure, microstructure and mechanical features of ceramic products of clay and non-plastic clay mixtures from Tunisia. Applied Clay Science, 135, 112-118.